Chapter 3

Colour-redshift classification of EROs

The last two decades have revealed a growing diversity of the extremely red galaxy population. Their extremely red colours, $R-K \geq 5$ or $I-K \geq 4$, constrain the possibilities essentially to three distinct galaxy types. Elliptical or dusty starburst galaxies in the high redshift regime (Pozzetti and Mannucci 2000, Pierini et al. 2004, Cimatti et al. 2002a) and normal spiral galaxies at similar redshifts (Gilbank et al. 2003, Moustakas et al. 2004), the separation between these galaxy types is a nontrivial task. Nevertheless, in order to test the various theories of galaxy formation, it is of great importance to understand the nature of EROs, especially whit respect to the applied colour criteria.

Every star has a specific colour determined by its spectral type, mass, age, and the abundance of heavy metals. Thus, multicolour photometry of a galaxy gives us information about the stellar populations, star formation, and the evolution of the galaxy. Based on the large variation in each of these parameters, the colour wavers from one galaxy to another even for galaxies of the same Hubble type. Nevertheless, using integrated colours, we can observe the effects of galaxy evolution. In order to understand the integrated colours of galaxies and interpret them in terms of star formation history and evolution, it is necessary to try to reproduce the actual spectral energy distribution (SED) for different Hubble types with theoretical models of galaxy evolution.
How do physical parameters, like age and metallicity, affect observable quantities such as colour and luminosity?

In this chapter, I will explore the possibilities for a galaxy to have an observed colour of $R-J \geq 5$, based on models for elliptical, dusty starburst, and normal spiral galaxies. The synthetic galaxy spectra are obtained using the spectral evolution synthesis code PÉGASE.2 (see Fioc and Rocca-Volmerange 1997).
Essentially two question will be addressed:

- What qualifies a member of the three galaxy populations as an ERO?
- How do parameters like Initial Mass Function (IMF), formation redshift, and initial metallicity influence the colour evolution?

In addition to the variable parameters, there are a number of factors which are common

to all models and which are listed in Table 3.1.

Property	Value
Mass range	$0.09 \leq M/M_{\odot} \leq 120$
Supernova ejecta	Woosley & Weaver (1995)
Infall	No
evolution of stellar metallicity	consistent
galactic winds	No
nebular emission	Yes
mass fraction of substellar objects	0.0

Table 3.1: PÉGASE.2 parameter common to all models.

In order to model the expected colours for our data set, I have added the transmission functions of the specific filter (Figure 3.1) to the filter set provided by PÉGASE.2. Although the specified J-band filters sample slightly different wavelength intervals, the R-J colours agree within 0.05 magnitudes (see Figure 3.2), which is approximately the accuracy of the R-band zero-point. In the course of modelling various galaxy formation scenarios, I will treat both filters as equal. Nevertheless, one has to be careful with assuming this for different filter bands.

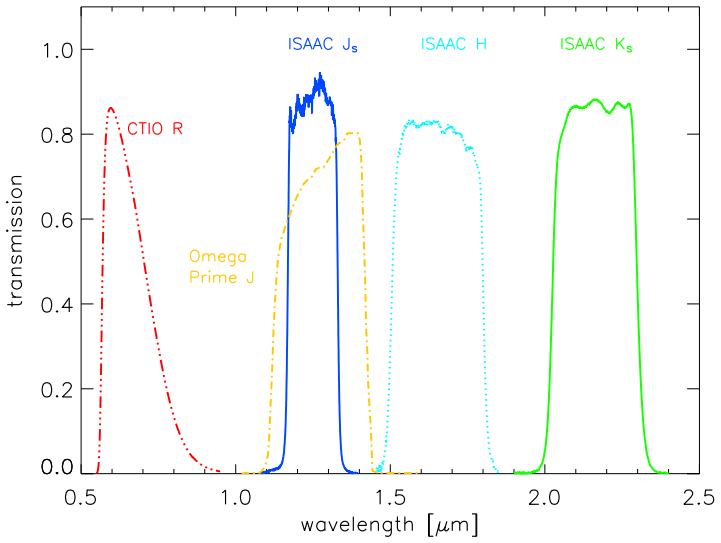

Figure 3.1: Transmission curves of the used VLT/ISAAC filers (J_s, H and K_s), the J-band filter from OMEGAPrime on Calar Alto and the R-band filter of the Prime Focus CCD Direct Camera at CTIO (note that this instrument is no longer available). The ISAAC filter are used for the models tested against the photometric separation from evolved ellipticals and dusty starbursts (see section 3.4 Figure 3.16).

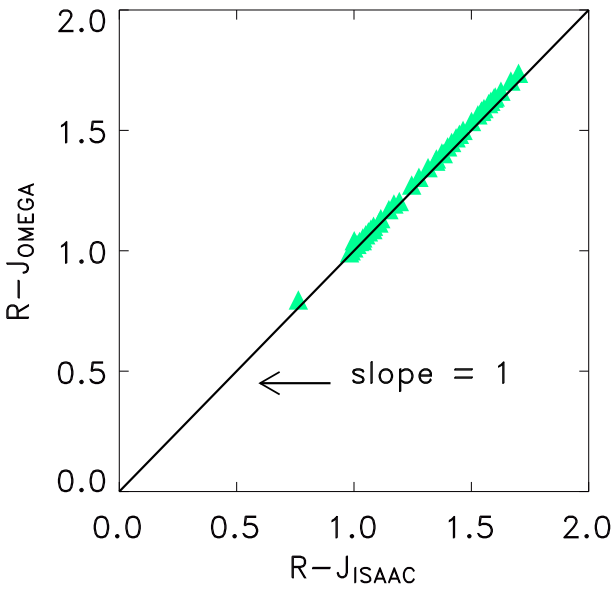

Figure 3.2: The influence of different J-band filters on R-J colours is negligible small. If not stated otherwise, we will use the colours based on the OMEGAPrime J-band filter.

3.1 Spectral energy distribution and colours of elliptical galaxies

Elliptical galaxies are modelled as galaxies that either evolve passively after an instantaneous burst of star formation, as described by eq. 3.1, or show an exponential decay in their star formation rate (SFR), mathematically expressed by eq. 3.2.
Instantaneous bursts are particularly suitable to test the impact of different evolutionary scenarios on spectral synthesis, since the spectra and colours are not smoothed by convolution with the SFR.

$$\text{instantaneous burst:} \qquad SFR(t) = \delta(t) \tag{3.1}$$

$$\text{exponential decay:} \qquad SFR(t) = \frac{A}{B}\, exp\left(\frac{-t}{B}\right), \quad \frac{A}{B} = SFR(t=0) \tag{3.2}$$

After the burst, the galaxies may still contain a certain amount of dust, which implies that we need to correct for extinction. The extinction by dust depends both on the spatial distribution of dust and stars and on its composition, related to the metallicity of the ISM. In the case of elliptical galaxies, we have applied the extinction correction for a spheroidal geometry, provided by PÉGASE.2.
We also tested parameters, such as the time of the last instantaneous burst (referred to as the formation redshift) and the initial metallicity, for their influence in reddening an elliptical galaxy enough to satisfy the R-J$\geq$5 colour criterion.
Additional to each specific scenario, we observe a general trend of the R-J colour to increase with age. The explanation for this can be seen in Figure 3.3: comparing the SED of elliptical

galaxies after 125, 1000 and 5000 M yr of passive evolution, the integrated luminosity sampled by the R band filter decreases with age. This is simply explained by the decreasing number of hot and massive stars producing the ultraviolet and optical flux of the SED.

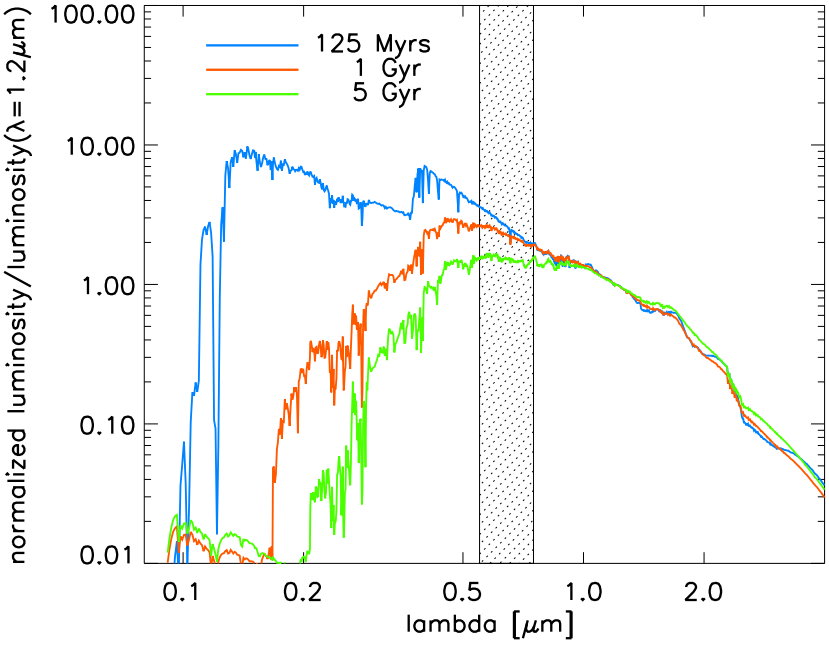

Figure 3.3: SED for an elliptical galaxy assuming Salpeter IMF and solar metallicity of the interstellar medium (ISM), normalised in the J band. The shadowed area indicates the wavelength range sampled by the R band filter. Due to the decreasing number of hot stars, the galaxy becomes redder with age.

3.1.1 Initial Mass Function

Modelling the different evolutionary scenarios begins with the assumption of an initial mass function $\xi(M)$ for a given mass range (see Table 3.2). In this chapter, we will explore the sensitivity of stellar synthesis models, assuming either a "present-day" Kroupa IMF (eq.6 in Kroupa 2001), a Scalo IMF (1998) or a Salpeter IMF (1955). The Kroupa IMF is mainly based on the power-law compilation by Scalo (1998), but the effects of unresolved binaries are also taken into account.
In order to separate the influence of the IMF from all other parameters we have neglected any extinction correction, thereby assuming a dust free galaxy. As was to be expected, Kroupa and Scalo IMFs result in an almost identical SED (Figure 3.5), whereas the Salpeter IMF shows a slightly redder SED. A possible explanation is the extrapolation of the Salpeter IMF to lower masses, where it is steeper than the Kroupa and Scalo relations. As a result, we would expect more low mass stars and a redder SED.
Nevertheless, the effect of the IMF compared to an "environmental" parameter like extinction geometry is negligible. Therefor we used a Salpeter IMF for all further modelling.

		=	$M^{-0.8}$	$0.08 \leq M/M_\odot <$	0.5
Kroupa IMF (Kroupa 2001)	ξ(M)	=	$M^{-1.7}$	$0.50 \leq M/M_\odot <$	1.0
		=	$M^{-1.3}$	$1.00 \leq M/M_\odot <$	∞
		=	$M^{-0.2}$	$0.10 \leq M/M_\odot <$	1
Scalo IMF (Scalo 1998)	ξ(M)	=	$M^{-1.7}$	$1.00 \leq M/M_\odot <$	10
		=	$M^{-1.3}$	$10.0 \leq M/M_\odot <$	100
Salpeter IMF (Salpeter 1955)	ξ(M)	=	$M^{-1.35}$	$0.4 \leq M/M_\odot <$	100

Table 3.2: Power law exponents for various Initial mass functions and their valid mass ranges (Figure 3.4.

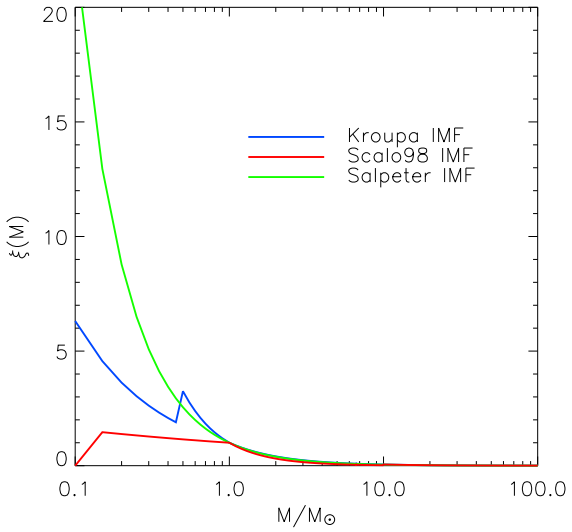

Figure 3.4: The initial Mass Function (IMF). The mass is given in multiples of one solar mass.

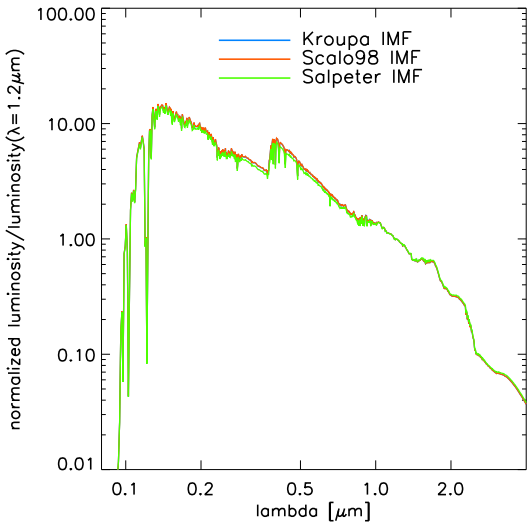

Figure 3.5: Spectral energy distributions of galaxies with different IMF's 125 Mio years after the burst, normalised in the J band. I assume the initial metallicity to be solar metallicity($Z_\odot$)= 0.02 and a mass range of $0.09 \leq M/M_\odot \leq 120$ for all models. The SED for a Kroupa IMF is identical to the Scalo IMF and cannot be distinguished. Extinction is not included.

3.1.2 Initial Metallicity and Formation redshift

Two close related parameters of star formation are age and the initial metallicity of the interstellar medium, from which each new stellar population is formed. Both factors result in a general reddening of the integrated colour. Assuming an instantaneous burst at a certain redshift allows us to separate the effect of these parameters without being affected by ongoing star formation.
Keeping the initial metallicity constant but having the galaxy formed at higher redshift, we can observe the effect of stellar aging. Vise versa, a constant formation redshift reflects solely the influence of the initial metallicity of the IMS one the colour evolution.

The R-J colour for different formation redshifts (z_f=2...7) and initial metallicities (Z=0.02..2.5$Z_\odot$) appear in Figure 3.6.
The results clearly show that it is very difficult for an elliptical galaxy to become redder than R-J$\geq$ 5. For metallicities below 0.2$Z_\odot$, not even the highest formation redshifts will yield red enough galaxies. A decreasing z_f, requires a higher limiting metallicity for an ERO, although if z_f=2, none of the assumed metallicities produces an ERO. Generally speaking, the ERO-producing range of metallicity and formation redshift is rather small. Solar metallicity of the ISM and a formation redshift of z_f=3 are required to redden a galaxy sufficiently to be classified as an ERO at one point during its evolution.
In additional to the above requirements, we can identify a redshift range and both lower and upper age limits for this EROs population (Tabele 3.3).

z_f	metallicity $Z/Z_\odot$	z_l	z_u	age_{zu}/Gyrs	age_{zl}/Gyrs
3	2.5	1.50	2.25	0.76	2.09
5	2.5	1.45	4.00	0.36	3.17
5	1.0	1.80	2.40	1.53	2.41
7	2.5	1.40	6.70	0.04	3.70
7	1.0	1.60	6.30	0.11	3.22

Table 3.3: Age and redshift intervals in which a galaxy satisfies an $R-J \geq 5$ colour criterion after an instantaneous burst of star formation. The intervals depend on the formation redshift and initial metallicity. According to the chosen cosmology the age of the universe is 13.5 Gyrs.

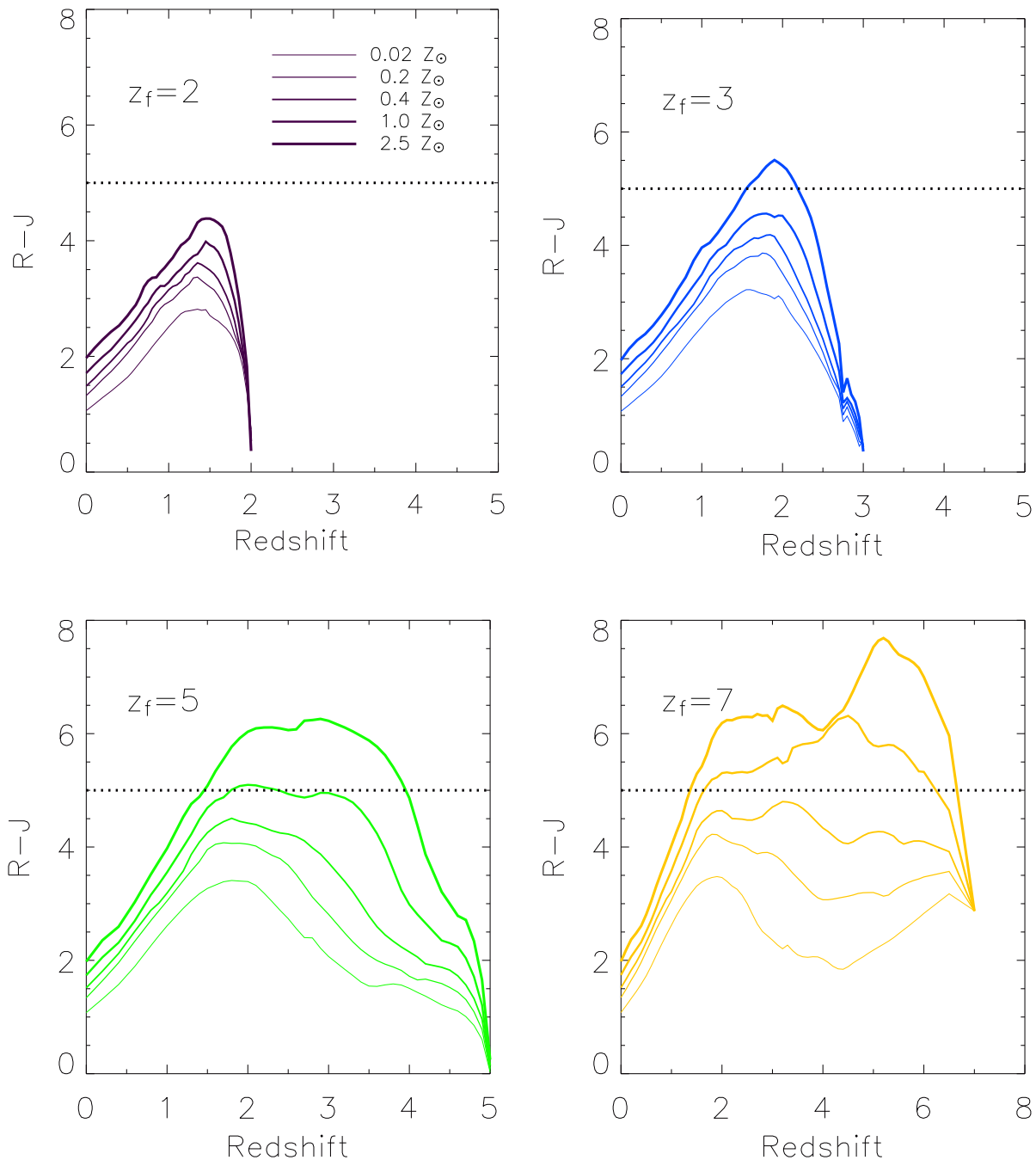

Figure 3.6: Colour-redshift diagrams for ellipticals of Salpeter IMF, assuming formation redshifts from 2 to 7 using the full range of initial metallicities (0.02,0.2,0.4,1 and 2.5 $Z_{\odot}$). The thickness of the lines increases according to the metallicity.

3.1.3 Influence of the Star Formation Rate

All previous models are based on the assumption that after an instantaneous burst, the galaxy forms no new stars. In reality there might be some star formation at later times, with a SFR which is probably not constant but declining until the galaxy evolves only in luminosity (Figure 3.7). For instance, a merger event or the accretion of material from tidally disrupted companions (Figure 3.8) can support the formation of new stars over some time.

The SFR at t=0 and decay-time scale were chosen in such a way that the star formation could continue over a time scale longer than the time between formation redshift and z=0. Hence, when the star formation stops, the galaxy might still contain a certain amount of dust. Table 3.4 shows the parameters relevant to the star formation history: initial SFR and decay-time.
Figure 3.9 shows the evolution of the R-J colour for different formation redshifts and, including the instantaneous burst scenario with an initial solar metallicity. However, if the last burst of star formation started at z=2 the galaxy does not redden sufficiently to be classified as an ERO. For increasing z_f, the limiting ERO-producing decay-time increases up to τ= 100 Mio years. If the star formation lasts longer than 500 Myr, not even the highest formation redshift will yield red enough galaxies.

z_f	SFR(t=0) ‡	τ [Myr]	z_l	z_u	age$_{zu}$/Gyrs	age$_{zl}$/Gyrs
3	0.10	10	1.50	2.20	0.82	2.09
3	0.02	50	1.50	2.20	0.82	2.09
3	0.01	100	1.50	2.10	0.96	2.09
5	0.10	10	1.45	3.45	0.65	3.17
5	0.02	50	1.45	3.40	0.68	3.17
5	0.01	100	1.45	3.00	0.96	3.17
7	0.10	10	1.45	6.50	0.08	3.57
7	0.02	50	1.45	4.70	0.49	3.57
7	0.01	100	1.45	3.80	0.86	3.57

Table 3.4: Age and redshift intervals in which a galaxy with exponential decreasing star formation rate satisfies the $R-J \geq 5$ colour criterion. The intervals depend on the formation redshift, initial star formation rate and decay-time. According to the chosen cosmology, the age of the universe is 13.5 Gyrs.

Figure 3.9 and Table 3.4 emphasise that with increasing decay-times, the redshift intervals in which EROs can be found become shorter. Longer decay-times imply prolonged star formation, i.e. during this time, the galaxy contains a number of newly born, hot and massive stars, whose ultraviolet/blue radiation compensates for the overall aging. Once star formation ends, one sees again the aging of the stellar populationpure luminosity evolution dominates the colour evolution. As expected, the colour then becomes independent of the initial star formation scenario. The colour evolution for these scenarios is not only the result of aging but also of the higher initial metallicity of the newly born stars (as discussed in section 3.1.3. This might explain the slightly redder R-J colours, even if the stellar population after an instantaneous burst is in average younger than after the burst.

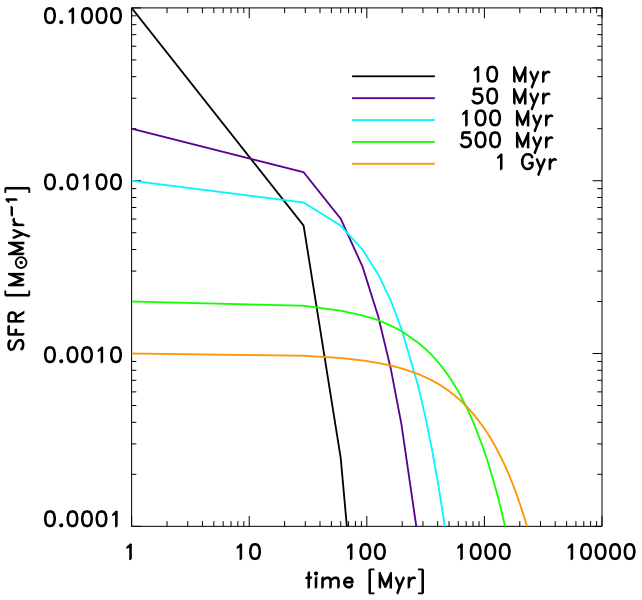

Figure 3.7: Star formation rate versus decay- time for an exponential decreasing SFR. The decay- time increases from 10 Myrs to 1 Gyr. The initial star formation rates are given in Table 3.5.

decay-time τ/ Myr	SFR(t=0) ‡
10	0.100
50	0.020
100	0.010
500	0.002
1000	0.001

Table 3.5: Initial SFR for starburst galaxies. The SFR for a real galaxy has to be multiplied by its total mass.

Figure 3.8: Multicolour composite of an ongoing merger and tidal interaction between two ellipticals (centre) and a spiral galaxy. The image was provided by the GEMS group.

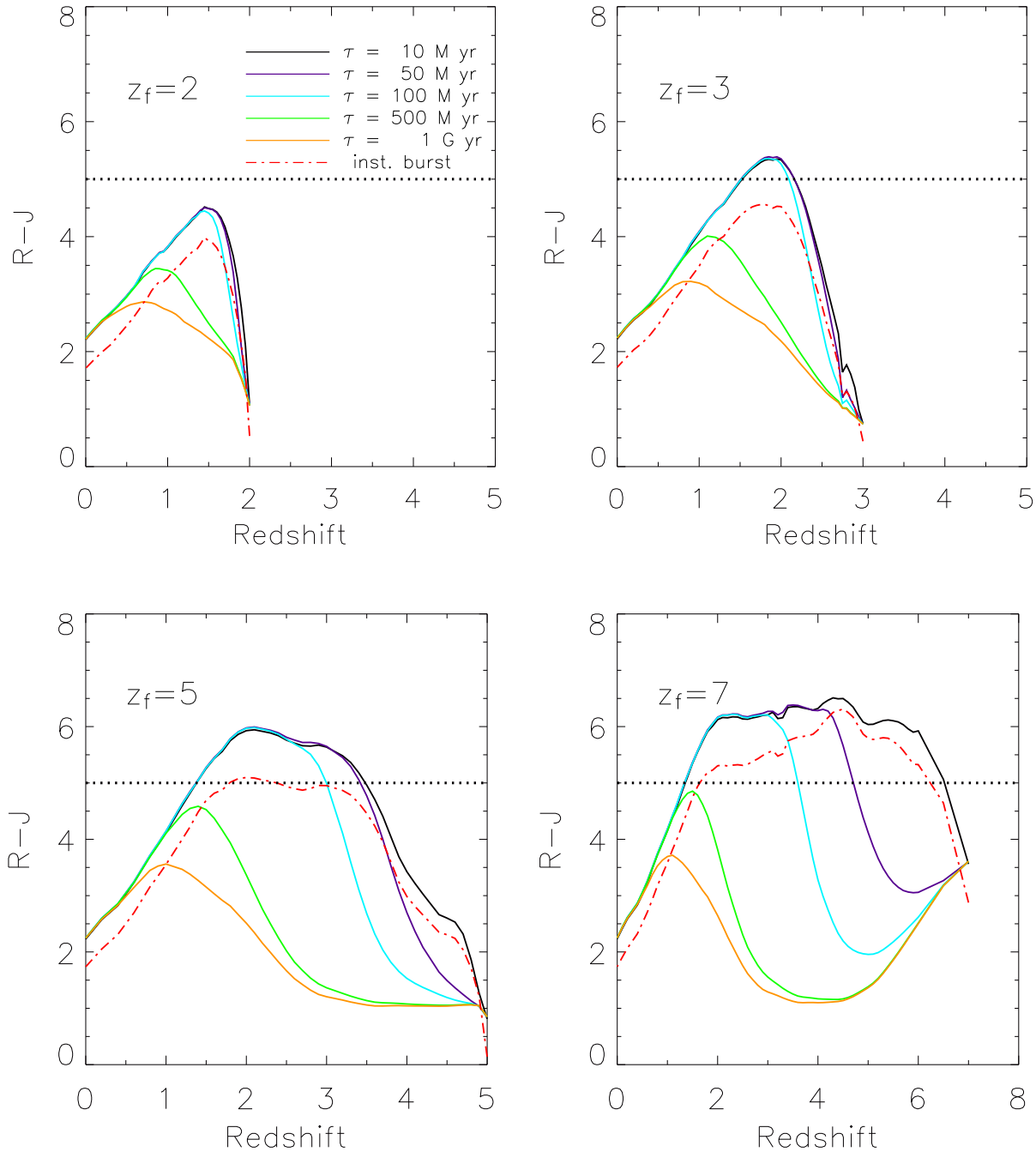

Figure 3.9: Colour-redshift diagrams for galaxies with an exponential decaying SFR. The colours reflect the same decay-time as in Figure 3.7. The dashed line shows the evolution for an instantaneous burst. All models assume an initial metallicity of $Z_{\odot}$ and Salpeter IMF. Also included is dust extinction for a spheriodal geometry.

3.2 Starburst Galaxies

ERO samples based on a R-K≥5..6 selection contain a substantial fraction of dusty starburst galaxies (Brusa et al. 2002, Cimatti et al. 2002a). These were modelled with a Salpeter IMF and constant star formation during 100 Myr (Bergström and Wiklind 2004,Heckman 1998). The extinction is naively treated as a uniform screen of dust and gas in the line of sight (see Figure 3.10). The amount of extinction is determined by the optical thickness of this dust layer. We have kept the colour excess (E(B-V) variable, in order to test which colour excess is needed for a starburst to qualify as ERO.
In the course of this work, we apply the extinction laws by Calzetti et al. (2000).

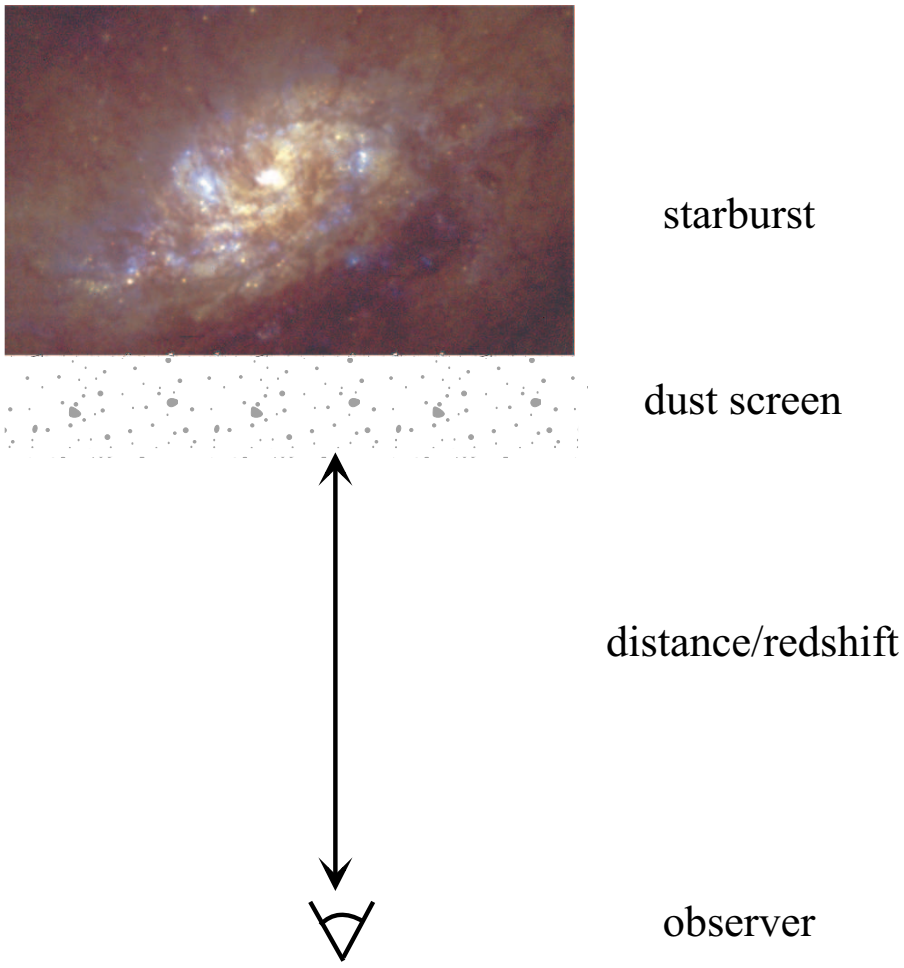

Figure 3.10: Sketch of the modelled extinction for a starburst galaxy. The extinction results from a dust layer between galaxy and observer, assumed to be at the same redshift as the galaxy

The stellar emission is calculated using the starburst reddening curve :

$$k(\lambda) \quad = \quad A'(\lambda)/E_s(B-V) \tag{3.3}$$

and an equation describing the relation between the observed $F_o(\lambda)$ and intrinsic $F_i(\lambda)$ stellar continuum flux densities.

$$F_o(\lambda) \quad = \quad F_i(\lambda)10^{-0.4E_s(B-V)k(\lambda)} \tag{3.4}$$

Due to different stellar environments and according to Calzetti et al. (2000), the stellar continuum and the nebular emission lines require a different extinction correction. Nevertheless, the colour excess of the stellar continuum $E_s(B-V)$ is linked to the colour excess derived from the nebular emission lines $E(B-V)$ by:

$$E_s(B-V) \quad = \quad 0.44\ E(B-V) \tag{3.5}$$

The wavelength dependent term $k(\lambda)$ is given by:

$$k(\lambda) \quad = \quad \begin{cases} 2.659(-2.156 + \frac{1.509}{\lambda} - \frac{0.198}{\lambda^2} + \frac{0.011}{\lambda^3}) + R_V & 0.12\mu m \leq \lambda \leq 0.63\mu m \\ \\ 2.659(-1.857 + \frac{1.040}{\lambda}) + R_V & 0.63\mu m < \lambda \leq 2.20\mu m \end{cases} \tag{3.6}$$

with $R_V = 4.05$ (Calzetti et al. 2000).

The PÉGASE.2 code allows an arbitrary value of the SFR, as long as it does not exceed the total mass of the galaxy. Nevertheless, a realistic SFR requires some preliminary considerations.

- The SFR provides only a scaling to the flux of the stellar spectrum. This scaling has no influence on the colours, as these are derived from the shape of the spectrum and not its absolute value. This also holds for the nebular emission lines, since the stellar continuum and emission lines are both proportional to the number of produced stars. Therefore, two galaxies of equal metallicity, formation redshift, IMF, and duration of star formation will have the same colour, regardless of the magnitude of the SFR.

- The SFR will influence the enrichment of the galaxy with heavy elements: the higher the SFR the faster the enrichment. This will definitely cause a change in colour.

As a result, only the increase in metallicity due to star formation has an effect on the colour, a fact we know from the colour evolution of elliptical galaxies.
Since consistent evolution of the metallicity is used in the modelling, the metallicities will change if the galaxy experiences a prolonged period of star formation. Therefore, the SFR is chosen in such a way that the metallicities do not differ too much from the initial metallicities. As with elliptical galaxies modelled, initial metallicities are 0.02, 0.2, 0.4, 1 and 2.5 $Z_\odot$.
Using a SFR of 5 x $10^{-5} M_\odot yr^{-1}$ per solar mass, ensures such a moderate enrichment during the 100 Myr of star formation. This SFR seems low, 25 $M_\odot yr^{-1}$ for a galaxy with a total mass of 5 x $10^{11} M_\odot$. However, since the magnitude of the SFR does not influence the colours of galaxies of the same metallicity and stellar population, this low SFR is equivalent

$Z_o/Z_\odot(t=0)$	Z_o(t=0)	$Z_e/Z_\odot$(t=100Myr)	Z_e(t=100Myr)	ΔZ[%]
0.02	0.0004	0.0238	0.000476	19.0
0.20	0.0040	0.205	0.0041	2.50
0.40	0.0080	0.405	0.0081	1.25
1.00	0.0200	1.005	0.0201	0.50
2.50	0.0500	2.505	0.0501	0.20

Table 3.6: Change of metallicity in the interstellar medium (ISM) after 100 Myr of constant star formation. SFR = 5x10$^{-5} M_\odot yr^{-1}$.

to models having a more "realistic" SFR. As far as the burst age is concerned, the assumed 100 Myr are longer than the estimate for the classical starburst (M82, Förster Schreiber et al. 2003), but agrees well with longer estimates of $\sim 10^7 - 10^8$ yr often quoted for starburst systems (e.g. Heckman 1998).
Considering the metallicity in the interstellar medium, an initial metallicity of 2.5Z$_\odot$ has increased to 2.505Z$_\odot$, i.e. by 0.2%, after 100 Myr. The heavy element enrichment is stronger for lower initial metallicities. For a starburst of initial metallicity 0.02Z$_\odot$, the increase is strongest, approximately 19% with respect to the initial value (Table 3.6).

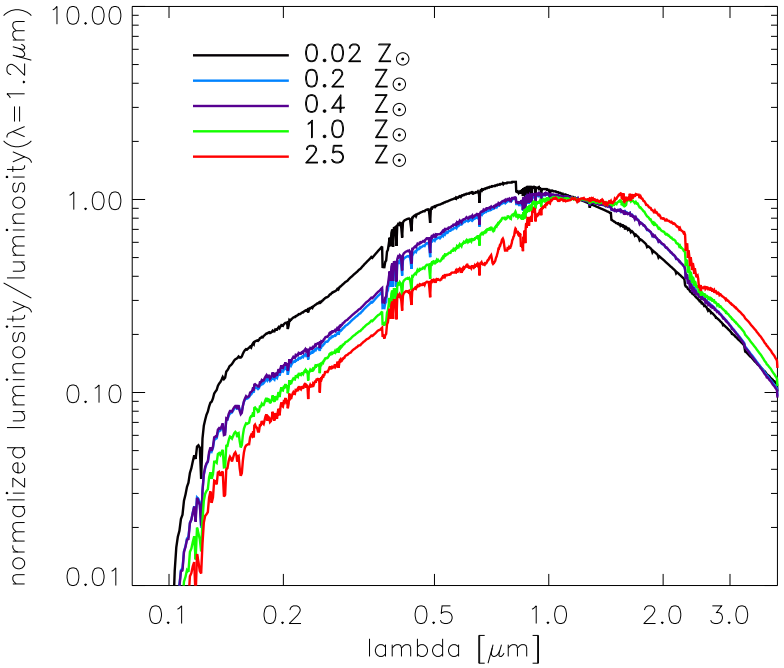

Figure 3.11: Spectral energy distribution of modelled starburst galaxies after 100 Myr of constant star formation. All models apply the same initial parameters, except metallicity, and an E(B-V)=2.0. The spectra are normalised to each other in the J band.

Figure 3.11 shows the spectral energy distribution of the starburst galaxies. The blue luminosity excess, powered by massive, hot stars, depends strongly on the initial metallicity, since higher metallicities produce more massive and shorter-lived stars. After 100 Myr, the number of hot stars in a galaxy with higher initial metallicity is small compared to the low metallicity galaxy, causing the SED to be redder.

The colour evolution for starburst galaxies of 0 and 100 Myr age, and the full range of metallicities are shown in Figure 3.12. The intermediate time steps would fill the colour space in between.
The colour-redshift plot shows some interesting features, especially the jumps in R-J around redshift 0.4, 0.8 and 1.5. From the stellar continuum alone, these discontinuities are not physical. The explanation are emission lines. For a specific redshift, these lines lie in the J band, e.g. H_α at 12000Å for z=0.8 and H_β at 12000Å for z=1.5.

For starburst galaxies, the evolution of R-J colour with redshift puts some constraints on the amount of reddening needed to produce an ERO. The limiting amount of extinction decreases as metallicity grows, since a more metal-rich galaxy will be redder. Nevertheless, even with $E(B-V) = 3.0$, a starburst has to be formed at redshift 4 or higher to be classified as an ERO.

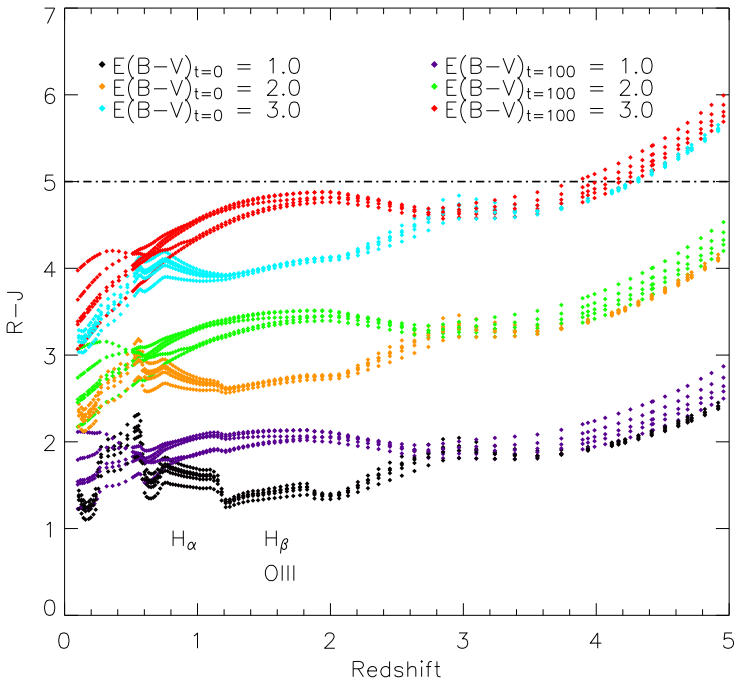

Figure 3.12: Colour-redshift diagram for starburst galaxies. The initial metallicities range from $0.02Z_\odot$ up to $2.5Z_\odot$. Curves of the same colour show the evolution for the whole range of metallicities. The discontinuities at certain redshifts can be explained by the luminosity contribution of individual emission lines.

Less strict colour criteria (R-K≥5, 5.3, or 6, Cimatti et al. 2002a, Roche et al. 2003, Thompson et al. 1999), sample both old ellipticals, starburst or spiral galaxies (Moustakas et al. 2004, Yan and Thompson 2003). The results of such a colour selection, e.g number count distribution, clustering behaviour, volume density of EROs, have to be interpreted in terms of containing different classes of EROs. So far, only evolved systems, which have been formed at redshift 3 or higher contribute to our ERO population.
Using a colour selection of R-J≥5, prevents starburst galaxies from being classified as an ERO. The possible contribution of spiral galaxies to our ERO sample will be discussed in the next chapter.

3.3 Spiral galaxies

In addition to the more "classical" ERO populations, recent high-resolution imaging with the HST have revealed a galaxy population at redshift z∼1, which also has very red optical-to-near-infrared colours: disk-dominated galaxies (e.g. Moustakas et al. 2004).

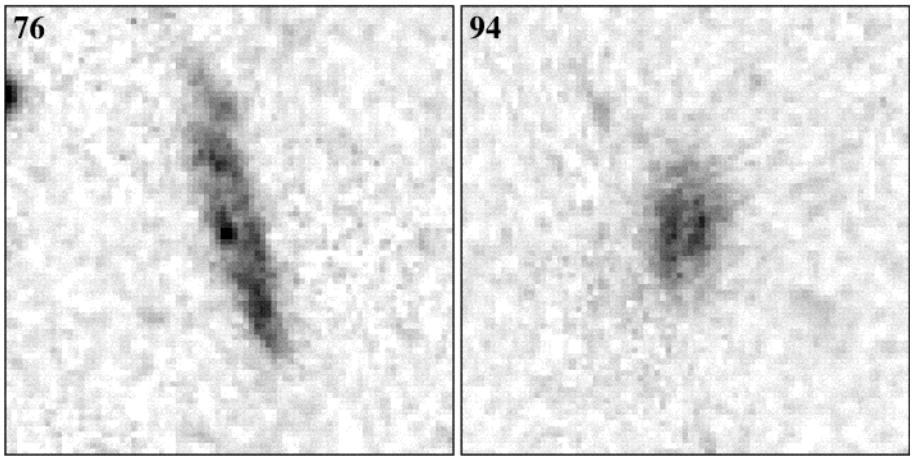

Figure 3.13: Two examples of disk dominated extremely red galaxies ($F814 - K_s \geq 4$). Due to their edge-on orientation, large amounts of dust lie in the line of sight, reddening the otherwise normal spiral galaxies. Both images are from Yan & Thompson 2003.

Due the limited resolution of our data-set, it is unlikely that we can detect disk structures. Nevertheless, in order to do a wide test on possible ERO populations ($R-J \geq 5$), we included disk galaxies in the PÉGASE.2 models.
These were modelled either with a constant star formation (like starburst galaxies) or with an exponentially declining star formation rate (elliptical galaxies). The basic model parameters are listed in Tab 3.7.

Figure 3.14 shows the colour evolution of a galaxy with disk geometry. The extinction was modelled both for an edge-on orientation (dashed line) and for non-zero inclination (solid line). A disk galaxy with a constant or slowly-decaying star formation rate has neither enough

Property	Value
Initial mass function	Kennicutt (1983)
Mass range	$0.09 \leq M/M_{\odot} \leq 120$
Star formation scenario	constant SFR
	exponential decay
orientation	inclination averaged
	edge-on
Formation redshift	1,2,3,5
Initial metallicity	$1Z_{\odot}$

Table 3.7: PÉGASE.2 parameter for modelling spiral galaxies.

dust nor a large enough fraction of old stars, to satisfy our $R - J \geq 5$ colour threshold. The detection of spiral galaxies as ERO seems to require a less red colour criteria, like I-K>4 (Yan and Thompson 2003, Gilbank et al. 2003).

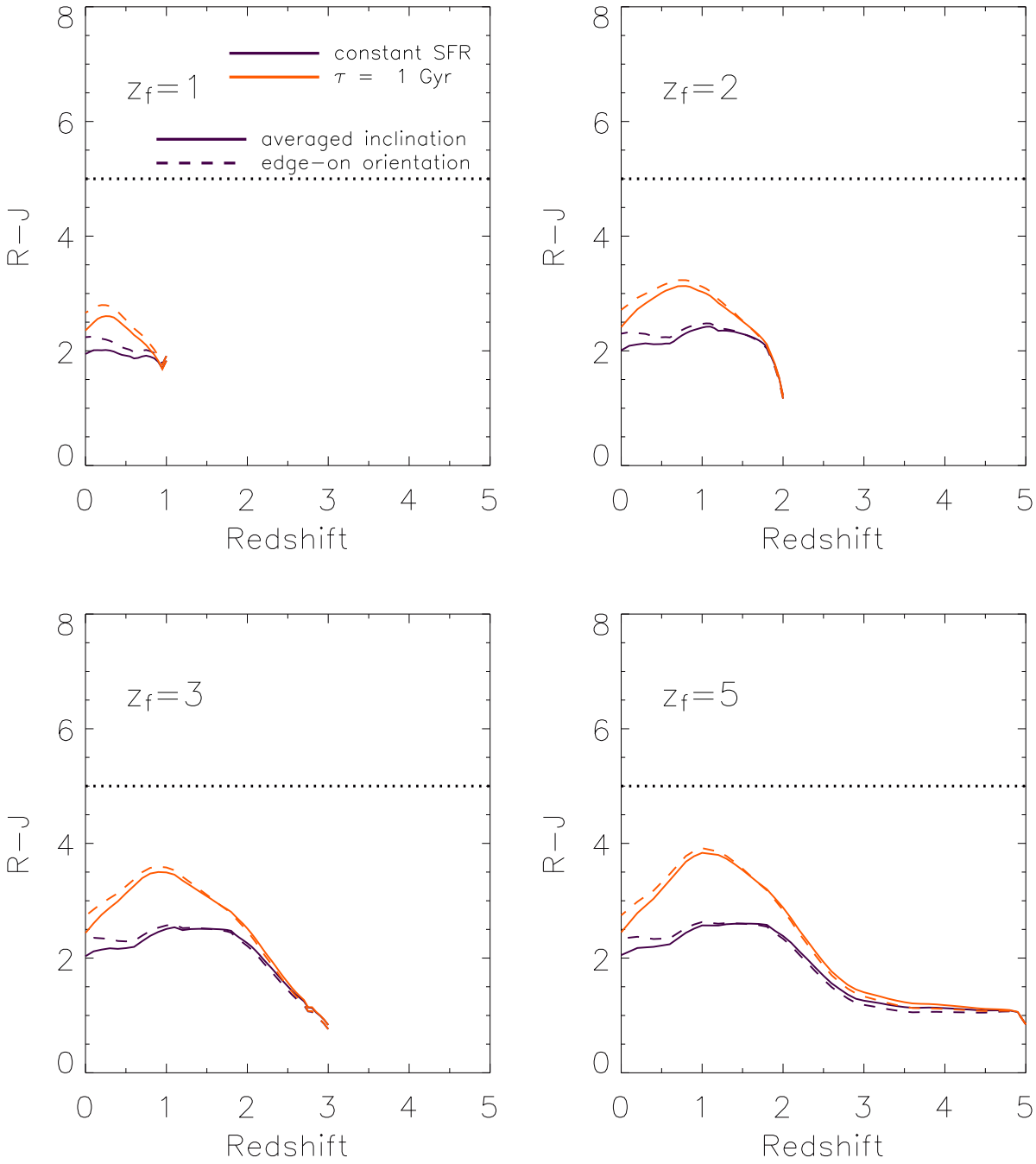

Figure 3.14: Colour-redshift diagrams for "normal" spiral galaxies. The solid lines represent an inclination-averaged orientation, while the dashed lines show the colour evolution assuming an edge-on geometry. Dust extinction is calculated in respect to the chosen geometry.

3.4 Possible candidates for EROs

The previous sections describe a number of stellar evolution models which have been tested for their ability to produce a galaxy with an optical to near-infrared colour of $R-J \geq 5$. Compared to less strict colour criteria, e.g. $R-K \geq 5$, the selection is limited almost exclusively to elliptical galaxies which contain an old stellar population. Figure 3.15 combines all models which produce EROs and allows the following conclusions regarding the ERO population:

Elliptical Galaxies

- The stellar population of an elliptical galaxy has to be formed at redshift $z_f \geq 3$ and is not picked up by our colour cut below redshift 1.4 (Figure 3.15).
- The initial metallicity of the ISM is approximately $Z_{\odot}$ or higher.
- The star formation history can be described either by:
  - an instantaneous burst, **or**
  - exponential decaying star formation rate with an decay-time $\tau \leq 100$ Myr.

Starburst Galaxies

- Starburst galaxies have to be formed at redshift $z_f \geq 5$ **AND**
- lie at $z \geq 4$ **AND**
- have an extinction of $E(B-V) \geq 3$, in order to be an ERO.

Disk Galaxies

- Disk galaxies contain neither enough dust nor a substantial fraction of old stars which could redden their spectral energy distribution enough, to classify these galaxies as EROs.

A sample of galaxies with colours redder than R-J$\geq$ 5 selects only one class of galaxies: ellipticals with an evolved stellar population. Since these galaxies have to be formed at high redshifts (z_f>3), they are good tracers of galaxy formation in early times.

As our modells have shown, only evolved ellipticals can be red enough to satisfy our colour criteria, R-J$\geq$5. Hence, each modelled galaxy with R-J$\geq$ 5 should be classified as elliptical using the proposed methods of photometric separation between old ellipticals and dusty starbursts.
Therefor, we used the results of the stellar population code to investigate how robust the calculated separation of Berström & Wiklind (2004) and Pozzetti & Mannucci (2000) between ellipticals and dusty starbursts is, if we apply those on the modelled ERO population. Figure 3.16 shows the colour-colour diagrams for all models which result in a $R-J \geq 5$ colour. The dashed lines indicate the separation between the two populations, with starburst galaxies

having the redder J-K or H-K colour. Figure 3.16 shows, that all EROs with $R - J \geq 5$ have blue enough near-infrared colours (either J-K or H-K) if they fall in the specified redshift range. Nevertheless, Figure 3.15 showed that EROs can be found in a much wider redshift interval, hence making the discrimination between the two ERO populations more difficult. Only the distribution in the R-H vs. H-K (Bergström and Wiklind 2004) is narrow enough to confine elliptical galaxies clearly from the starburst colour space. Even if the colour excess increases, it will result only in a shift parallel to the separation line.

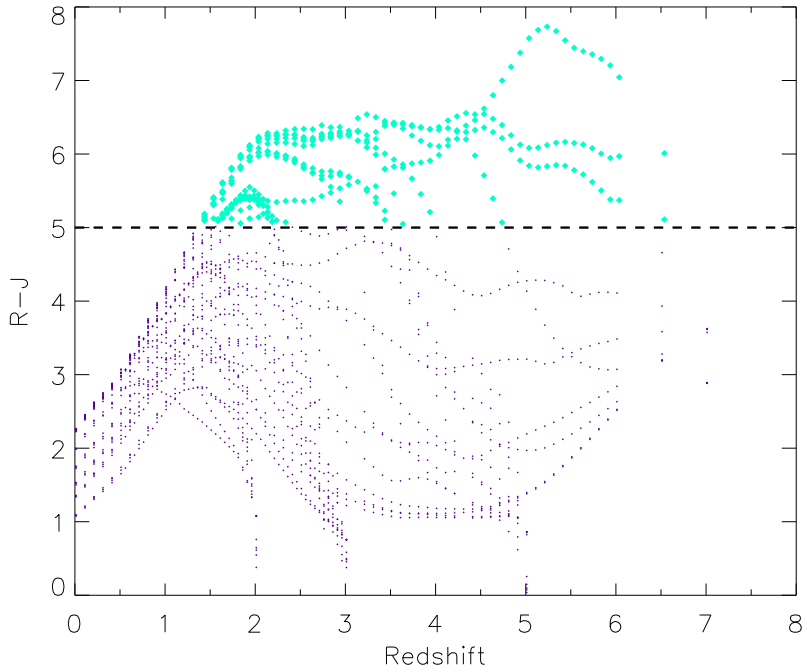

Figure 3.15: Colour-redshift diagram for all star formation scenarios of elliptical galaxies, which produce colours redder than $R - J \geq 5$ (see section 3.1). The green dots highlight the colours above R-J>5.

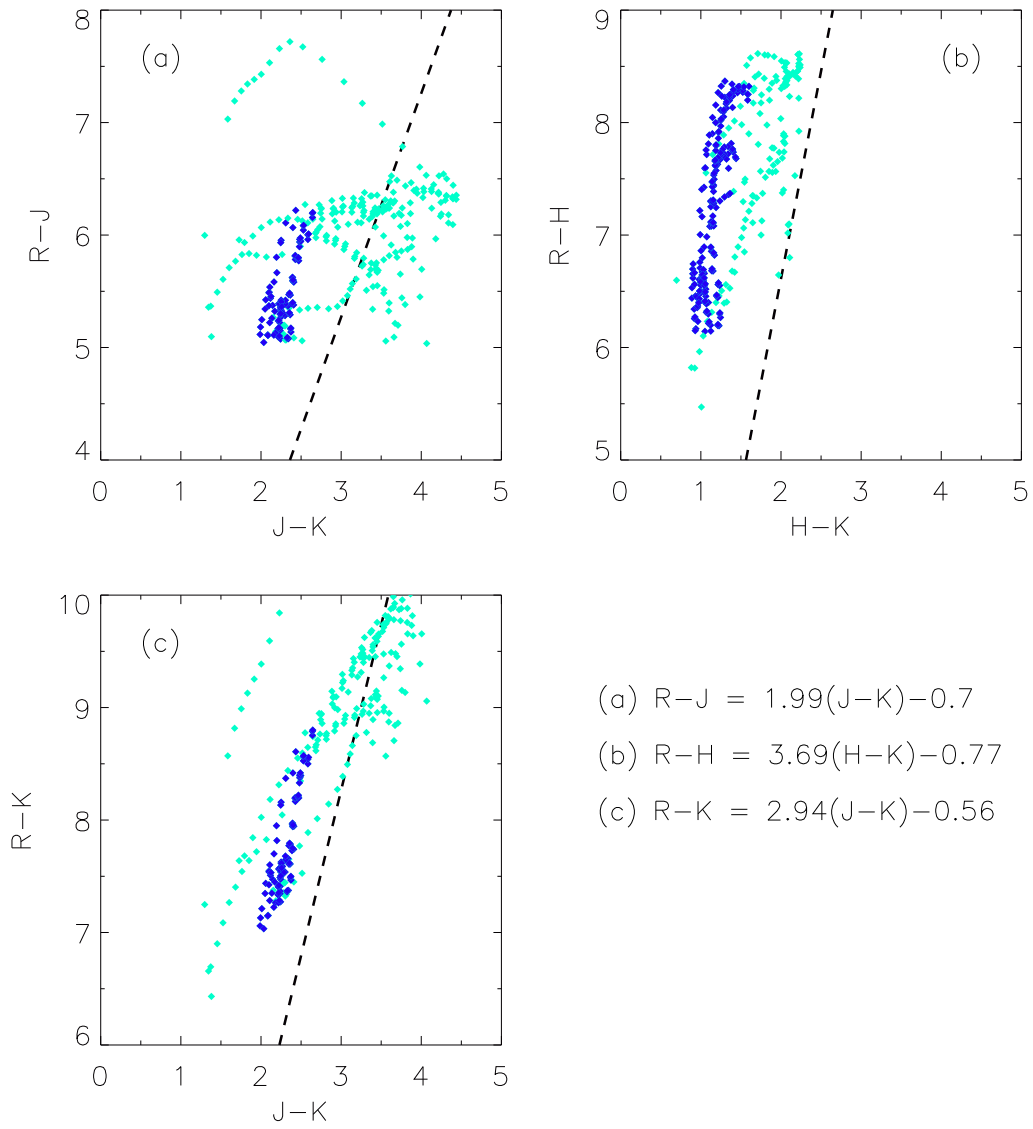

Figure 3.16: Colour-colour diagram for model galaxies having $R - J \geq 5$. The dashed lines show the separation between elliptical galaxies and starbursts, calculated by Bergström & Wiklind (panel (a) and (b), 2004) and Pozzetti & Mannucci (panel (c), 2000). The blue symbols mark objects with redshifts below 2.1 (a), below 3 (b) and between 1 and 2 (c), for which these separation lines where calculated.